A 1-DIMENSIONAL MODEL OF INDIRECT BIOMASS GASIFICATION IN A DUAL FLUIDISED BED SYSTEM

Louise Lundberg*, David Pallarès, Robert Johansson, Henrik Thunman

Department of Energy and Environment

Chalmers University of Technology, SE-412 96 Göteborg, Sweden

Email: louise.lundberg@chalmers.se*

Abstract –A 1-dimensional model is used to analyse how solids material circulation, biomass reactivity and gas mixing affect the char conversion in the Chalmers 2-4 MW indirect biomass gasifier. For the geometry and operational conditions particular to this unit, the model predicts a peak in char conversion for a solids circulation rate of around 3 kg/s. Char conversion is found to increase substantially with biomass reactivity and the level of gas mixing. At the experimental rate of solids circulation (6 kg/s), modelled char conversion values lie between 9% and 39% and are thus quite far from the experimental value of 2% (although potentially ranging between 0 and 10% due to experimental uncertainty). An explanation of the higher char conversion provided by the model could be the uncertainty in the reactivity of the biomass used. A further possible explanation, which has been studied by means of modelling in this work, is the gas mixing. The model uses expressions for the gas mixing which have been derived from measurements in smaller lab units with a high-pressure drop gas distributor, *i.e.* which induce a better gas mixing than the limited one existing in the large-scale unit studied here, caused by the presence of large bubbles and regions with weak fluidisation.

1. INTRODUCTION

Indirect biomass gasification in a dual fluidised bed system can be used to convert solid biomass into raw gas, which can be further upgraded for use as substitute natural gas, city gas, fuel in gas turbines or liquid transport fuels. The necessary heat to sustain gasification is supplied by the bed material, which circulates between the combustor and the gasifier. The circulating bed material also carries unconverted char from the gasifier to the combustor, playing a significant role on the char residence time in the gasifier (and the combustor). It thereby influences the share of char conversion taking place in the gasifier respectively combustor and the overall performance of the process.

The model presented here is the first milestone in the development of a 3-dimensional model to be used as a tool in the optimisation and up-scaling of the indirect gasification process. The modelling is carried out within the framework of the GoBiGas project in Göteborg (Sweden), in which a 20 MW demonstration plant was put into operation during 2013 and whose final aim is to produce biogas on a commercial scale (80-100 MW) by the end of this decade. Such large-scale indirect gasification processes achieve optimal performance when the degree of char conversion in the gasifier is in the range of 40-60% (Larsson *et al*., 2013), thus predictive modelling of char conversion is crucial for reliable design of the process.

This study is focused on the Chalmers dual fluidised bed system, which consists of a CFB combustor and a BFB gasifier, the latter operating continuously with a fuel input ranging between 2 and 4 MW, Fig. 1.

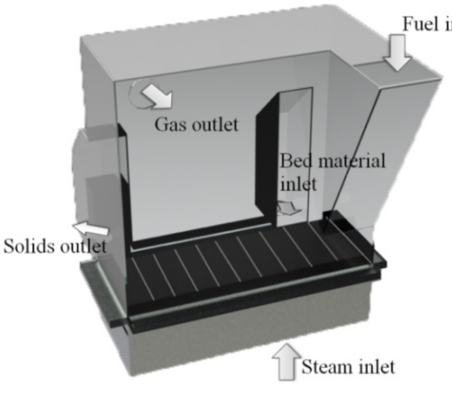

Fig. 1. Layout of the Chalmers gasifier, showing the direction of discretisation used in the 1D-model (white lines).

The present work aims at analysing how different parameters affect char conversion in indirect biomass gasification by means of a comprehensive 1-dimensional model. The influence of bed material circulation, biomass reactivity and gas mixing on the degree of char conversion are studied.

2. MODEL DESCRIPTION

In this work, the dense bed of an indirect biomass gasifier is modelled in one, the horizontal, dimension, Fig. 1. The model solves transport equations for energy and mass of inert solids, fuel at different stages of conversion (drying, pyrolysis and different degrees of char gasification) and the individual gas species (H_2O, CO, CO_2, H_2, CH_4, and tars lumped into C_6H_6O). The model includes submodels for homogeneous and heterogeneous kinetics and convective and dispersive mixing of gas species, fuel particles and bed material. A two-phase model is used to account for the gas mixing.

The boundary conditions used in this work are perfectly insulated walls and no mass flow through walls. The finite volume method is used to discretise the transport equations, using the hybrid scheme to estimate the properties at cell faces. Grid independency was checked and it was seen that 100 cells were sufficient to get a grid independent solution, so 100 cells were used in all the simulations.

2.1. Equations of the Solid Species

The transport equation for each component, *i*, of the fuel (ash, moisture, solid volatiles and char) is written as:

$$\frac{d}{dx}(\theta u_{BM}\rho_i) = \frac{d}{dx}\left(D_F\frac{d\rho_i}{dx}\right) + S_i \tag{1}$$

The term on the left hand side (LHS) represents mass transfer by convection, where θ is the cross-flow impact factor, an empirically derived coefficient describing how well the fuel particles follow the velocity field, u_{BM}, induced by the cross-flow of solids. $\theta = 1$ implies that the velocity of the fuel is equal to that of the bed material, whereas $\theta = 0$ implies that the fuel particles do not follow the cross-flow of solids at all. In this work θ is set to 0.9 (Larsson *et. al.* 2014). The first term on the right hand side (RHS) describes mass transfer by dispersion (with the lateral dispersion coefficient for the fuel set to 0.037 m^2/s, (Sette *et. al.* 2013)) and the last term is the source term, which differs for the different solid species (see Section 2.4).

In order to account for the influence of the size of the char particles on the rate of char conversion, the char is divided into a number of particle size classes, Fig. 2, with one mass balance being solved for each. During char gasification, particles of class *k* decrease in size which results in a flow, $\dot{n}_k$, of char into size *k-1*, Fig. 2. In the same way, conversion of particles of size *k+1* results in a flow, $\dot{n}_{k+1}$, of particles into class *k*. $\dot{n}_k$ is defined according to:

$$\dot{n}_k = \frac{\frac{dm_{CH,k}}{dt}}{V_{k,layer}\rho_c} \tag{2}$$

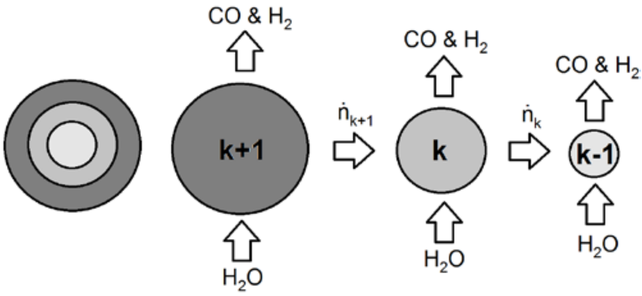

Fig. 2. Discretisation of the char conversion into size classes.

The velocity field induced by the cross-flow of the bed material circulating in the system is calculated by first assuming that the transport of bed material occurs through dispersive lateral mixing (Kunii and Levenspiel, 1991), with a source term, S_{BM}, accounting for the bed material inlet and outlet, Eq. 3. The solution of this equation yields a fictional bed material concentration gradient, $\frac{d\phi_{BM}}{dx}$, which is used to find the velocity field, Eq. 4. The actual concentration of bed material in the gasifier, ρ_{BM}, is assumed to be constant and the lateral solids dispersion coefficient for the bed material, D_{BM}, is taken as 0.015 m^2/s (Sette *et.al.* 2012).

$$0 = \frac{d}{dx}\left(D_{BM}\frac{d\phi_{BM}}{dx}\right) + S_{BM} \tag{3}$$

$$u_{BM} = \frac{D_{BM}}{\rho_{BM}}\left(\frac{d\phi_{BM}}{dx}\right) \tag{4}$$

Fragmentation and attrition of char particles are not taken into account in this work.

2.2. Equations of the Gas Species

As mentioned above, the gas flow is based on a two-phase flow model with an emulsion phase and a bubble phase including gas exchange between the phases (Toomey and Johnstone, 1952). The following assumptions are made:

- The emulsion phase consists of bed material, fuel particles and gas at minimum fluidisation conditions. The minimum fluidisation velocity is calculated using a correlation proposed by (Wen and Yu, 1966), yielding u_{mf} =3 cm/s. This gives the voidage at minimum fluidisation conditions as ε_{mf} =0.38, derived from the Ergun equation.
- The bubble phase consists exclusively of gas.
- Drying and pyrolysis takes place at the bed surface and the gases released are thus not considered to pass into the emulsion phase. This is in line with observations with a camera probe in the Chalmers gasifier in which drying and devolatilising fuel particles were observed to float on the surface of the dense bed, in agreement with the reported formation of endogenous bubbles at bubbling conditions which lift the fuel to the dense bed surface (Bruni *et. al.*, 2002).
- Gas dispersion between cells takes place in the emulsion phase only.

Mass balances for the gas species are set up for the bubble phase and the emulsion phase according to Eqs. 5 and 6 respectively. The gas exchange between the phases is governed by a mass transfer coefficient, K_{be}.

$$0 = K_{be}\left(\rho_{G,e}X_{e,j} - \rho_{G,b}X_{b,j}\right) + S_{b,j} \tag{5}$$

$$0 = -\frac{d}{dx}\left(D_G\rho_{G,e}\frac{dX_j}{dx}\right) - K_{be}\left(\rho_{G,e}X_{e,j} - \rho_{G,b}X_{b,j}\right) + S_{e,j} \tag{6}$$

The lateral dispersion coefficient for the gas, D_G, is taken as 10^{-4} m^2/s (Oka, 2004). The source term for the bubble phase, $S_{b,j}$ consists of gas species entering and exiting the gasifier in the bubble phase, as well as species being formed during homogenous reactions. For the emulsion phase, the source term, $S_{e,j}$, also accounts for species consumed and formed during char gasification.

2.3. Energy Equation

The solids are assumed to have the same temperature as the gas, which means that only one energy balance is solved:

$$\begin{aligned} C_{p,BM}\frac{d}{dx}(u_{BM}\rho_{BM}T) + \sum_i \frac{d}{dx}(\theta u_{BM}\rho_i h_i) &= -\sum_i \frac{d}{dx}\left((D_F h_i)\frac{d\rho_i}{dx}\right) \\ -\frac{d}{dx}\left((k+k')\frac{dT}{dx}\right) - \frac{d}{dx}\left(\sum_j\left(D_G h_j \rho_{tot}\frac{dX_j}{dx}\right)\right) + S_E \end{aligned} \tag{7}$$

The two terms on the LHS represent heat transfer by convection of bed material and the different components of the fuel. The fuel components are assumed to remain at the inlet temperature until they are converted into gas. Ash, however, is heated and is assumed to attain the same temperature as the bed.

The first term on the RHS describes heat transfer by dispersion of the different fuel species. The second term combines conduction, k, and heat transfer related to the dispersive mass transfer of bed material and ash, where k' is defined according to:

$$k' = D_{BM}C_{p,BM}\rho_{BM} + D_F C_{p,A}\rho_A \tag{8}$$

Heat transfer by gas dispersion is described by the third term on the RHS of Eq. 7. The source term, S_E, includes the feeding and removal of bed material and fuel, as well as the addition of steam and the raw gas leaving for the freeboard. Absolute enthalpy values are used for all species in Eq. 7, *i.e.* thereby including the heats of reaction.

2.4 Fuel Conversion

The shrinking particle model is used to describe char gasification:

$$\frac{dm_{CH,k}}{dt} = -\,\Omega A_{P,k} n_{P,k} k_{rc,eff,k} C_{H_2O,\infty} M_C \tag{9}$$

Where $k_{rc,eff}$ includes both diffusion of water vapour from the surroundings to the particle surface and kinetics:

$$k_{rc,eff} = \frac{k_{rc}h_m}{k_{rc} + h_m} \tag{10}$$

k_{rc} is given by an Arrhenius expression. Experiments for the determination of the reactivity of the present biomass are planned within short, but in the absence of reactivity data, the influence of biomass reactivity to H_2O is studied considering two values for the activation energy, E_A: 128.0 kJ/mole (Tamarin, 1991) and 157.6 kJ/mole, which represent biomass with high and low reactivity, respectively. These values fall within the range 105-270 kJ/mole considered standard for biomass fuels according to Barrio (2002). The pre-exponential factor is calculated as $10^{(0.2\cdot 10^{-4}E_A+2)}$ (Tamarin, 1991). The mass transfer coefficient, h_m, is calculated with a Sherwood correlation (Ranz, 1952):

$$Sh = \frac{h_m d_P}{D_{AB}} = \left(2 + 0.6Re^{0.5}Sc^{1/3}\right) \tag{11}$$

The drying and pyrolysis are described according to Eq. 12, with rate constants and reference values as specified in Table 1.

$$\frac{dm_{M/V}}{dt} = -k_{dt/pt}\frac{T}{T_{ref}}\frac{d_{P,ref}}{d_P}\rho_{M/V}\Delta V \tag{12}$$

Table 1. Rate constants and reference values used to model drying and pyrolysis (Larsson *et. al.* 2013).

$d_{p,ref}$	k_{dt}	k_{pt}	T_{ref}
1 cm	1/20 s^{-1}	1/45 s^{-1}	850 °C

The only homogenous reaction considered is the water-gas-shift reaction, with the parameters for the forward reaction rate and the equilibrium constant given by (Biba *et al.*, 1978) and (Kanury, 1977), respectively. The reactants within a phase are assumed to be well mixed.

3. RESULTS

Fig. 3 shows char conversion in the gasifier as a function of three parameters: the solids circulation rate, the reactivity of the biomass and the gas exchange coefficient between bubble and emulsion phase.

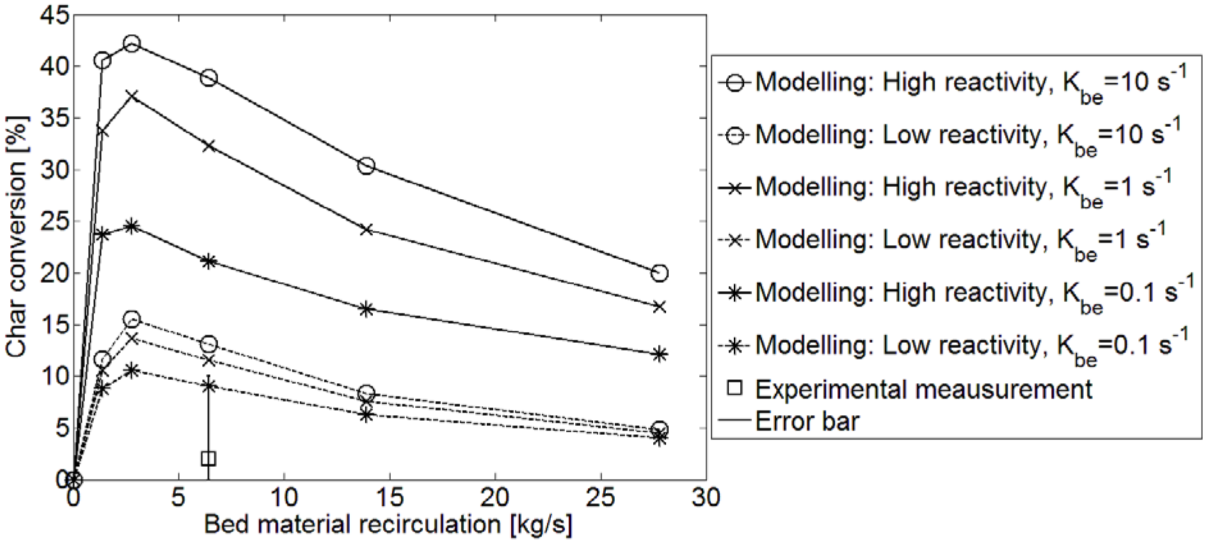

Fig. 3. Char conversion as a function of circulation rate of bed material for different biomass reactivities and extents of gas mixing.

The model predicts a char conversion peak at a solids circulation rate which for all cases is located around 3 kg/s. Solids circulation rates below this value decrease the heat carried by the bed material, which results in a lower temperature in the gasifier and thereby a lower char conversion. For higher solids circulation rates it is the shortened residence time of the char in the gasifier that leads to a decrease in char conversion.

The reactivity of the biomass also strongly influences the char conversion, as seen by comparing cases with high and low biomass reactivities in Fig. 3. The highly reactive biomass gives a significantly higher char conversion at all solids circulation rates studied. This indicates that the modelled results are rather sensitive to the choice of kinetic parameters, strengthening the relevance of a proper characterisation of the mechanisms of the char conversion.

Fig. 3 also shows that the gas mixing influences char conversion, especially for the biomass with high reactivity. Relatively high values of the mass transfer coefficient, K_{be}, above 1 s^{-1}, typical for lab units, yield a maximum char conversion of around 12% and 32% for the low respectively high reactivity of the biomass at the experimental solids circulation rate of 6 kg/s. Both these degrees of char conversion are far from the experimental value in the Chalmers gasifier of 0-10% (this range is caused by the following uncertainties: the measurements of the pyrolytic char yield, the amount of the carbon in the raw gas that origins from the flue gas and unburned char from the combustor and the carbon measurements of the raw gas) (Neves *et al.*, 2013), with the best estimate being 2%. As seen in Fig. 3, such low conversion degrees can be attained by the 1D model with values of K_{be} below 0.1 s^{-1}, or by further decreasing the reactivity of the biomass. Values for K_{be} as low as 0.1 s^{-1} are not found in literature, which is, however, limited to laboratory units with small bubbles. In large-scale units such as the one studied here, larger bubbles are formed, which yield lower values of the mass transfer coefficient (Kunii and Levenspiel, 1991 and Oka, 2004).

There are other possible reasons for the low char conversion observed experimentally, although they have not been studied in this work. The strongly heterogeneous char distribution at the bed surface observed with a hot camera probe indicates a limitation in the contact between steam and fuel particles and possibly also a decreased local concentration of steam due to the release of volatiles and product gases from the char gasification. Both these effects lower the effective steam concentration surrounding the biomass particles. Furthermore, the camera probe observations also show that some bed regions could be de-fluidised, thus having a steam flow through the emulsion lower than that at minimum fluidisation assumed in the present modelling, thus limiting fuel conversion.

4. CONCLUSIONS

A 1-dimensional model for indirect gasification has been developed which gives an insight in how operational parameters influence char conversion. Both biomass reactivity and solids circulation have a strong impact on the degree of char conversion, while the impact of gas mixing becomes more significant as the biomass reactivity increases. The model predicts the existence of a solids circulation rate maximising char conversion.

NOTATION

Roman uppercase letters

A_P	surface area of char particle (m^2)
$C_{H2O,\infty}$	steam concentration in gasifier ($mole/m^3$)
C_p	specific heat (J/kg/K)
D	dispersion coefficient (m^2/s)
D_{AB}	diffusion coefficient (m^2/s)
K_{be}	bubble-emulsion interchange coefficient (s^{-1})
M	molar mass (kg/mole)
S	source term (depends on balance)
T	temperature (K)
V	volume (m^3)
$V_{k,layer}$	volume of char layer of size class k (m^3)
X	gas species mass fraction

Roman lowercase letters

d_P	particle diameter (m)
k	total thermal conductivity (W/m/K)
k'	dispersion heat transfer coefficient (W/m/K)
k_{dt}	inverse of the time of evaporation (s^{-1})
k_{pt}	inverse of the time of pyrolysis (s^{-1})
k_{rc}	rate constant of char gasification (m/s)
$k_{rc,eff}$	effective rate constant of char gasification (m/s)
h	enthalpy (J/kg)
h_m	diffusion coefficient (m/s)
$m_{CH,k}$	mass of reacted char at size k per cell (kg/cell)
$\dot{n}_k$	flow of char particles out of class k (particles/s)
$n_{P,k}$	number of char particles of size k per cell

Greek letters

ε	bed voidage (-)
ρ	density or concentration in gasifier (kg/m^3)
ϕ	fictional bed material concentration (kg/m^3)
Ω	mole C/mole H_2O
θ	cross-flow impact factor (-)

Dimensionless groups

Sc	Scmidth number
Sh	Sherwood number
Re	Reynolds number

Subscripts

A	ash
b	bubble
BM	bed material
c	char particle
C	carbon
e	emulsion
E	energy
F	fuel
G	raw gas
i	fuel species
j	gas species
k	char size class
M	moisture
mf	minimum fluidisation

t	time (s)	ref	reference
u	velocity (m/s)	tot	total
x	dimension of discretisation (m)	V	solid volatiles

REFERENCES

Barrio, M. 2002. Experimental Investigation of Small-Scale Gasification of Woody Biomass. PhD thesis, Faculty of Engineering Science and Technology, Norwegian University of Science and Technology, Trondheim.

Biba, V., Macák, J., Klose, E., Malecha, J. 1978. Mathematical Model for the Gasification of Coal under Pressure. Industrial & Engineering Chemistry Process Design and Development 17, 92-98.

Bruni, G., Solimene, R., Marzocchella, A., Salatino, P., Yates, J.G., Lettieri, P., Fiorentino, M. 2002. Self-Segregation of High-Volatile Fuel Particles During Devolatilization in a Fluidized Bed Reactor. Powder Technology 128, 11-21.

Kanury, A.M. 1977. Introduction to Combustion Phenomena, Gordon and Breach, New York.

Kunii, D., Levenspiel. O. 1991. Fluidization Engineering, Butterworth-Heinemann, Newton.

Larsson, A., Seemann M., Neves, D., Thunman H. 2013. Evaluation of Performance of Industrial-Scale Dual Fluidized Bed Gasifiers Using the Chalmers 2-4MW$_{th}$ Gasifier. Energy and Fuels 27, 6665-6680.

Larsson, A., Sette, E., Breitholtz, C., Pallarès D., Seemann, M., Thunman, H. 2014. Increasing Char Conversion in a Dual Fluidized Bed Gasification System. To be submitted.

Neves, D., Thunman, H., Tarelho, L., Larsson, A., Seemann, M., Matosa, A. 2014. Method for Online Measurement of the CHON Composition of Raw Gas from Biomass Gasifier. Applied Energy 113, 932-945.

Oka, S.N. 2004. Fluidized Bed Combustion, Marcel Dekker Inc., New York.

Ranz, W.E. 1952. Friction and Heat Transfer Coefficient for Single Particles and Packed Beds. Chemical Engineering Progress 28, 247.

Sette, E., Aimé, S., Pallarès, D., Johnsson, F. 2013. Analysis of Lateral Fuel Mixing in a Fluid-Dynamically Down-Scaled Bubbling Fluidized Bed. Fluidization XIV.

Sette, E., Gómez García, A., Pallarès, D., Johnsson, F. 2012. Quantitative Evaluation of Inert Solids Mixing in a Bubbling Fluidized Bed. 21st International Conference on Fluidized Bed Combustion.

Tamarin, A.I. 1991. Model of Coal Combustion in a Fluidized Bed and its Experimental Identification. Journal of Engineering Physics and Thermodynamics, 60, 693-697.

Toomey, R.D., Johnstone, H.F. 1952. Gaseous Fluidization of Solid Particles, 48, 220-225.

Wen, C.Y., Yu, Y.H. 1966. A Generalized Method for Predicting the Minimum Fluidization Velocity. AIChE Journal, 12, 610-612.